DALTON
FULL PAPER

Control of molecular topology by stereochemical preferences of metal ions: double helical *versus* side-by-side structures in tetranuclear copper(II) and nickel(II) complexes †

Roland Krämer,* Igor O. Fritsky,‡ Hans Pritzkow and Larisa A. Kovbasyuk ‡

Anorganisch-Chemisches Institut, Universität Heidelberg, Im Neuenheimer Feld 270, 69120 Heidelberg, Germany

Received 21st August 2001, Accepted 11th February 2002
First published as an Advance Article on the web 6th March 2002

The novel polydentate ligand *N*,*N*′-bis(5-(2-pyridyl)-4*H*-pyrazole-3-carbonyl)-1,2-diaminoethane (**L**) was prepared in one-pot synthesis, employing Claisen condensation of 2-acetylpyridine and diethyl ethylene-1,2-bis(oxamate) followed by treatment with hydrazine hydrate. **L** possesses four bidentate chelating units and is expected to be able to bind metal ions in bis(binucleating) or tetradentate modes. Reaction of **L** with 1 equiv. of copper(II) or nickel(II) hydroxides in the presence of 2 equiv. KOH in DMSO affords mononuclear anionic complexes $K_2[(Cu(\mathbf{L} - 4H)]\cdot 5H_2O$ (**1**) and $K_2[(Ni(\mathbf{L} - 4H)]\cdot 6H_2O$ (**2**) containing metal ions in square-planar environment of two pairs of deprotonated amide and pyrazolato nitrogens. Reaction of **1** with 2 equiv. of $Cu(NO_3)_2$ leads to complete rearrangement of the coordination sphere, yielding a tetranuclear product which was crystallised in the presence of picric acid in the form $[Cu_4(\mathbf{L} - 2H)_2(DMSO)_2(EtOH)_2](picrate)_4$ (**3a**). Complex $[Cu_4(\mathbf{L} - 2H)_2(H_2O)_4](NO_3)_4\cdot 4H_2O$ (**3b**) was obtained as a result of spontaneous self-assembly from **L** and copper(II) nitrate in aqueous acetic acid. Reaction of **2** with 2 equiv. of $Ni(NO_3)_2$ yields a tetranuclear cationic complex $[Ni_4(\mathbf{L} - 2H)_2(DMSO)_6(NO_3)(H_2O)](NO_3)_3\cdot H_2O\cdot 3DMSO\cdot(CH_3)_2CO$ (**4**) which contains four octahedral Ni ions coordinated in bis(binucleating) mode to two ligand threads disposed in side-by-side fashion and *cis* with respect to the Ni(1)–Ni(2) axis. In both **3a** and **3b** the ligand is coordinated in the same bis(binucleating) mode as in Ni complex **4**, however, the Cu ions are square-pyramidal and the two ligand threads are disposed *trans* with respect to the Cu(1)–Cu(2) axis, thus giving rise to the double helical structures. **3a** and **3b** are the first examples of helicates comprising of bimetallic units. Formation of different topologies in **3a**,**b** and **4** is elucidated in terms of different stereochemical preferences of these ions in mixed N,O-donor environments. All compounds were characterised by elemental analysis, ESI and MALDI mass spectrometry and UV–VIS spectroscopy, and complexes **3a**, **3b** and **4** by single crystal X-ray analysis. Magnetic susceptibility measurements (1.7–300 K) of powdered samples of tetranuclear complexes revealed strong (**3b**) or moderate (**4**) antiferromagnetic coupling within the dimeric units incorporating double pyrazolato bridges between paramagnetic centres.

Self-assembly of polynuclear coordination compounds with predetermined topological architecture (*e.g.*, helicates, containers, grids, ladders) is based on various design principles, such as the use of ligands with certain arrangements of coordination compartments, variation of donor groups basicity, utilisation of specific stereochemical preferences of different metal ions as well as a variety of non-covalent interactions.[1] Helicates have been extensively investigated during the last decade,[1b,c] and the recognised approaches to such molecules imply the use of metal-ion induced self-assembly of ligand threads containing repeating donor units of certain denticity, so that the binding abilities of the ligand domains need to match to the stereochemical requirements of the metal ions.[1b,c,2,3]

We are currently interested in design of ligand systems capable to form polynuclear complexes which can provide adequate models for bimetallic active sites of metalloenzymes where the control of metal–metal separation and thus functional activity is modulated by presence of a third, allosteric metal ion.[4] In this context, we have prepared a new polynucleating ligand **L** (Scheme 1), and its mono- and poly-nuclear complexes. **L** has four bidentate chelating units: two {N(Py), N(Pz)} and two {N(Pz), (N or O)(amide)}. Interestingly, 3,5-substituted pyrazole derivatives have been successfully utilised both in complexes modelling bimetallic biosites and in synthesis of supramolecular coordination arrays.[5,6] While 3-(2-pyridyl)-pyrazolato ligands providing {N(Py), N(Pz)} chelating sites have been extensively studied and used, *e.g.*, for the synthesis of polynuclear assemblies with different topologies,[6] in particular, double helicates,[6b,c] the {N(Pz), N(amide)} donor set, is not well explored in this respect.[7] In the case of square-planar coordination of bivalent metal ion at the tetradentate site of **L**, the anticipated anionic complexes $[M(\mathbf{L} - 4H)]^{2-}$ (Scheme 2, upper part) carrying two {N(Py), N(Pz)} chelating units are expected to be able to bind one or two extra metal ions. This possibility would require retaining the square-planar $M_s\{2N(Py), 2N(Het)\}$ core in the polynuclear complex. On the other hand, the coordination behaviour of the amide group is ambiguous. On protonation of the amide groups, the ligand would be coordinated in a bis(binucleating) mode with a long spacer between the chelating units resulting in sophisticated polynuclear arrays. We established that realisation of certain molecular topologies in this case is dictated by specific stereochemical requirements of the metal ions.

Experimental

All chemicals were commercial products of reagent grade and used without further purification. ^{1}H NMR spectra were recorded on Bruker AC-400 (400.13 MHz) and Bruker AC-500

† Dedicated to Prof. Dr Walter Siebert on the occasion of his 65th birthday.
‡ On leave from Department of Chemistry, Shevchenko University, 01033 Kiev, Ukraine.

DOI: 10.1039/b107593b

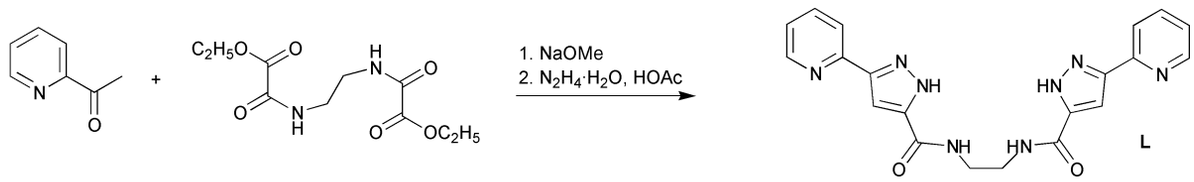

Scheme 1 Synthesis of ligand **L**.

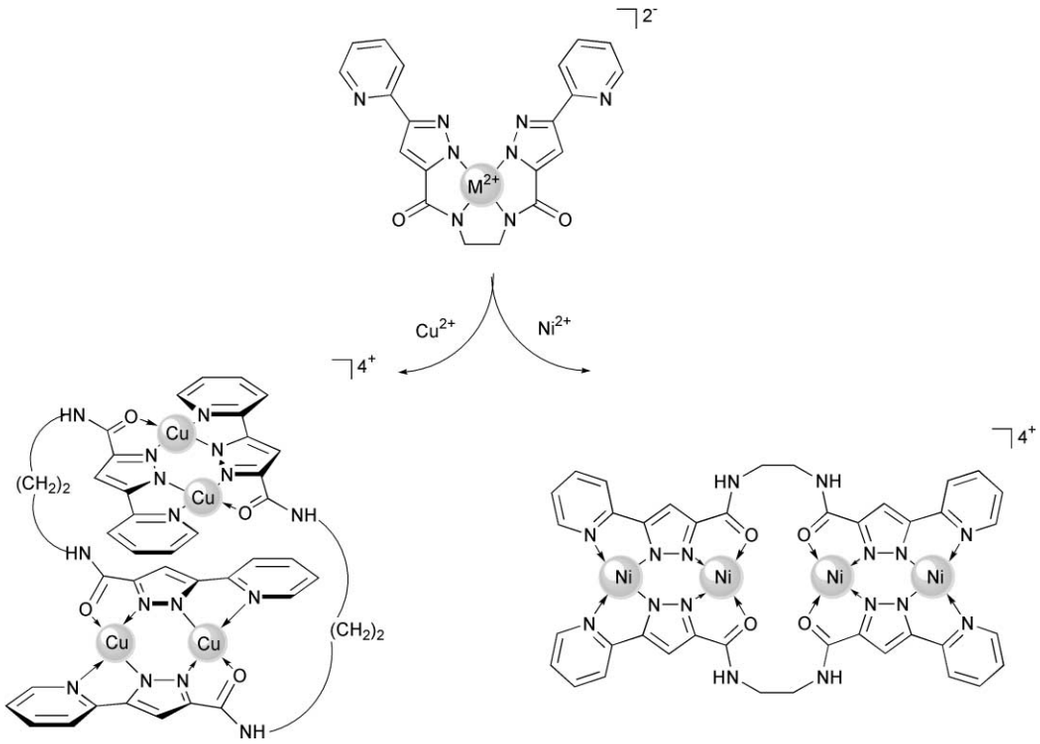

Scheme 2 Rearrangement of mononuclear $[M(\mathbf{L} - 4H)]^{2-}$ into tetranuclear $[M_4(\mathbf{L} - 2H)_2]^{4+}$ on uptake of extra metal ions.

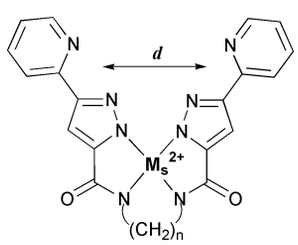

(500.15 MHz) spectrometers, chemical shifts are reported in ppm downfield from Me_4Si. Field desorption (FD) mass spectra were recorded with a JEOL JMS-700 instrument, electrospray (ESI) mass spectra were obtained on a Finnigan TSQ 700 device. IR spectra (KBr pellets) were recorded on a Perkin-Elmer 983 G spectrometer. Absorbance UV–VIS spectra of solutions were registered on a Specord S100 spectrophotometer (Carl Zeiss Jena). The EPR spectra of solid samples and frozen solutions were recorded on a Bruker ESP 300E spectrometer at X-band (9.3 GHz) at 120 and 300 K. Variable-temperature magnetic susceptibility data (1.7–300 K) were acquired on powdered samples with use of a Quantum Design MPMS-5 SQUID magnetometer. Corrections for the diamagnetism of the ligand were applied using Pascal's constants and the diamagnetic contribution from the sample holder was also taken into account. Elemental analyses were conducted by the Microanalytisches Laboratorium des Organisch-Chemischen Instituts der Universität Heidelberg.

Preparations

***N*,*N*′-Bis(5-(2-pyridyl)-4*H*-pyrazole-3-carbonyl)-1,2-diaminoethane (L).** Sodium methylate (30% solution in methanol, 3.6 g, 0.02 mol) was added dropwise with stirring to a mixture of 2-acetylpyridine (2.42 g, 0.02 mol) and the diethyl ester of ethylene-1,2-bis(oxamic acid) (2.60 g, 0.01 mol, prepared according to ref. 8) in 20 ml of absolute ethanol at 0 °C. The resulting suspension was stirred for 12 h at room temperature, then the formed pale yellow precipitate was collected by filtration, washed with ethanol and immediately suspended in 50 ml of ethanol. 2 ml of glacial acetic acid and 1.5 ml of hydrazine hydrate were added subsequently, and the mixture was collected by filtration and refluxed for 3 h. After cooling, the formed white precipitate was filtered off, washed with water and ethanol and dried *in vacuo*. Yield 2.94 g (73%). Elemental analysis (%): calc. for $C_{20}H_{18}N_8O_2$ (402.42): C 59.69, H 4.51, N 27.85; found: C 59.45, H 4.39, N 27.98; FD-MS, *m*/*z* (%): 403.4 (100, M + H^+); IR, cm^{-1}: 771, 999, 1265, 1549 (Amide II), 1661 (C=O Amide I), 3301 (N–H); ^{1}H NMR (400.13 MHz, DMSO-d_6), δ 3.45 (br s, 4H, CH_2), 7.34 (s, 2H, Pz-4), 7.35 (m, 2H, Py-5, $J_{4,5}$ = 7.8, $J_{5,6}$ = 4.8 Hz), 7.88 (td, 2H, Py-4, $J_{3,4}$ = 7.8, $J_{4,6}$ = 1.2 Hz), 7.95 (m, 2H, Py-3), 8.50 (br s, 2H, NH), 8.62 (m, 2H, Py-6), 13.87 (s, 2H, Pz-1,2); ^{13}C NMR (DMSO-d_6), δ C(N–CH_2) overlap with DMSO peak, 104.7 (Pz-4), 121.1 (Py-3(?)), 124.1 (Py-5(?)), 138.2 (Pz-3(?)), 143.8 (Pz-3(?)), 148.3 (Py-4(?)), 148.4 (Py-6(?)), 150.1 (Py-2(?)), 162.6 C(C=O).

K_2[(Cu(L − 4H)]·5H_2O (1) and K_2[(Ni(L − 4H)]·6H_2O (2). To **L** (0.201 g, 0.5 mmol) dissolved in 15 ml DMSO 1 ml of 1 M aqueous KOH was added at 80 °C with stirring. To the obtained solution, freshly prepared copper(II) or nickel(II) hydroxide (for **1** and **2**, respectively, obtained by addition of 1.2 ml of 1 M aqueous KOH to 0.5 ml of 1 M aqueous $Cu(NO_3)_2$ or $Ni(NO_3)_2$) was added. The obtained mixture was stirred at 80 °C for 10 min. The resultant purple (Cu) or orange–yellow (Ni) solutions were cooled, filtered and the solvent was distilled off

in vacuo. Obtained powders were washed with acetone and dried *in vacuo*.

1: Yield 0.296 g (94%). Elemental analysis (%): calc. for $C_{20}H_{14}N_8O_2CuK_2\cdot 5H_2O$ (630.20): C 38.12, H 3.84, N 17.78; found: C 38.09, H 3.96, N 17.50; UV/Vis (DMSO), λ_{max}/nm (ε/dm^3 mol^{-1} cm^{-1}): 508 (307); ESI-MS, *m*/*z* (%): 230.2 (100, $[^{63}Cu(\mathbf{L} - 4H)]^{2-}$), 462.0 (31, $[^{63}Cu(\mathbf{L} - 3H)]^{-}$).

2: Yield 0.290 g (90%). Elemental analysis (%): calc. for $C_{20}H_{14}N_8O_2NiK_2\cdot 6H_2O$ (643.36): C 37.34, H 4.07, N 17.42; found: C 37.61, H 3.93, N 17.21; UV/Vis (DMSO–H_2O, 3 :2), λ_{max}/nm (ε/dm^3 mol^{-1} cm^{-1}): 423 (sh) (307); ESI-MS, *m*/*z* (%): 228.1 (100, $[^{58}Ni(\mathbf{L} - 4H)]^{2-}$).

$[Cu_4(\mathbf{L} - 2H)_2(DMSO)_2(EtOH)_2](picrate)_4$ (3a) and $[Ni_4(\mathbf{L} - 2H)_2(DMSO)_6(NO_3)(H_2O)](NO_3)_3\cdot H_2O\cdot 3DMSO\cdot(CH_3)_2CO$ (4). To **L** (0.201 g, 0.5 mmol) dissolved in 15 ml DMSO, 2 ml of 1 M aqueous KOH and then 0.5 ml of 1 M aqueous $Cu(NO_3)_2$ or $Ni(NO_3)_2$, for **3a** and **4**, respectively, were added at 80 °C and the solution stirred for 10 min.

3a. To the resulting solution 0.5 ml of 1 M aqueous $Cu(NO_3)_2$ solution and 2 ml of 1 M ethanol solution of picric acid and then isopropanol (20 ml) were added. Blue crystals were grown within 48 h. Elemental analysis (%): calc. for $Cu_4C_{72}H_{64}N_{28}O_{36}S_2$ (2215.77): C 39.03, H 2.91, N 17.70; found: C 39.19, H 2.85, N 17.88.

4. To the resulting solution 1 ml of 1 M aqueous $Ni(NO_3)_2$ solution was added. Single crystals of complex were obtained by slow diffusion of acetone vapour to the resulting solution at room temperature. Elemental analysis (crystals lose solvate acetone in the air) (%): calc. for $Ni_4C_{58}H_{90}N_{20}O_{27}S_9$ (2022.77): C 34.44, H 4.48, N 13.85; found: C 34.21, H 4.55, N 13.98; UV/Vis (DMSO), λ_{max}/nm (ε/dm^3 mol^{-1} cm^{-1}): 586 (11.5), 754 (sh) (13), 846 (23); ESI-MS, *m*/*z* (%): 515.0 (100, $[\{^{58}Ni_2(\mathbf{L} - 2H)\} - H]^+$), 517.0 (71, $[\{^{58}Ni^{60}Ni(\mathbf{L} - 2H)\} - H]^+$), 519.0 (27, $[\{^{60}Ni_2(\mathbf{L} - 2H)\} - H]^+$), 1029.0, 1031.0, 1033.0, 1035.0 (minor peaks, $[\{Ni_4(\mathbf{L} - 2H)_2\} - 3H]^+$).

$[Cu_4(\mathbf{L} - 2H)_2(H_2O)_4](NO_3)_4\cdot 5.5H_2O$ (3b). To **L** (0.201 g, 0.5 mmol) suspended in 15 ml of 10% aqueous acetic acid and heated to 80 °C, 1 ml of 1 M copper(II) nitrate aqueous solution was added. The mixture was heated with stirring for *ca.* 30 min. The resulting clear solution was filtered and set aside for crystallisation at room temperature. Blue–green prismatic crystals of the complex were obtained in 36 h, filtered and air-dried. Yield 0.246 g (68%). Elemental analysis (%): calc. for $Cu_4C_{40}H_{51}N_{20}O_{25.5}$ (1474.15): C 32.59, H 3.49, N 19.00, Cu 17.24; found: C 32.94, H 3.43, N 19.08, Cu 17.56; UV/Vis (H_2O), λ_{max}/nm (ε/dm^3 mol^{-1} cm^{-1}): 607 (115); UV/Vis (DMSO), λ_{max}/nm (ε/dm^3 mol^{-1} cm^{-1}): 607 (152), 320 (5945); ESI-MS, *m*/*z* (%): 351.0 (100, $[\{^{63}Cu_3{}^{65}Cu(\mathbf{L} - 2H)_2\} - H]^{3+}$), 526.0 (20, $[\{^{63}Cu_3{}^{65}Cu(\mathbf{L} - 2H)_2\} - 2H]^{2+}$), 1051.0 (15, $[\{^{63}Cu_3{}^{65}Cu(\mathbf{L} - 2H)_2\} - 3H]^+$).

X-Ray crystallography

Details of the crystal data and refinement are given in Table 1. Intensities were collected using a Bruker AXS CCD Smart 1000 diffractometer with graphite-monochromated Mo-Kα radiation (λ = 0.71073 Å) (for **3b**: P_4 Bruker diffractometer in the θ–2θ scan mode). Corrections for Lorentz and polarization effects were applied. Absorption corrections were performed by a semi-empirical method based on multiple scans of equivalent reflections using the SADABS routine.[9] The structures were solved by direct methods (SHELXS-97)[10] and refined by full-matrix least-squares (SHELXTL NT V.5.1.)[11] anisotropically for all non-hydrogen atoms. Aromatic and aliphatic C–H hydrogen atoms (excluding the methyl hydrogen atoms of disordered or half-occupancy DMSO and acetone molecules of **4**) were placed on calculated positions and were allowed to ride on the atoms to which they were connected. In **3a** and **3b**, N–H and O–H hydrogen atoms (excluding several hydrogen atoms of water molecules in **3b** which have not been observed) were located from the difference Fourier map and refined isotropically, in **3a** the ethanol O–H hydrogen atom was located but not included into refinement. In **4** the N–H hydrogen atoms were located from the difference Fourier map but not included into further stages of refinement. Significant disorder was found in one of the coordinated DMSO molecules and a non-coordinated nitrate anion in **4**. The coordinated nitrate anion in **4** was observed with occupancy factor of 0.53, and one of its oxygens was found to share the same space with the oxygen of the coordinated water molecule of 0.47 occupancy. There are also disordered solvate DMSO and acetone molecules in **4**. There is a disordered water molecules region in the structure of **3b**.

CCDC reference numbers 171613–171615.

See http://www.rsc.org/suppdata/dt/b1/b107593b/ for crystallographic data in CIF or other electronic format.

Results and discussion

The novel conformationally flexible polydentate ligand **L** was prepared with good yield (73%) in one-pot synthesis, employing Claisen condensation of 2-acetylpyridine and diethyl ethylene-1,2-bis(oxamate) in the presence of sodium ethylate in anhydrous ethanol, followed by treatment of the obtained sodium salt of bis(amido-β-diketone) with acetic acid and hydrazine hydrate in ethanol under reflux (Scheme 1). The synthesis does not require isolation of the intermediate bis(amido-β-diketone). It is worthwhile to note that this is a rare example of the use of amidoesters in Claisen condensation,[12] and this approach, in our opinion, can be successfully expanded for a variety of amido-β-diketones and polynucleating hetaryl-carboxamide ligands.

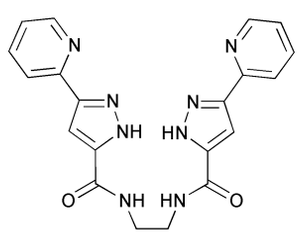

As expected, **L** interacts readily with Ni^{II} and Cu^{II} nitrates in 1 : 1 molar ratio in DMSO in the presence of 4 equiv. of base (KOH), producing $[M(\mathbf{L} - 4H)]^{2-}$ ($M = Cu^{2+}$, Ni^{2+}). Formation of doubly-charged mononuclear anionic species was detected by ESI mass spectroscopy: both spectra exhibit peaks corresponding to $[Ni(\mathbf{L} - 4H)]^{2-}$ and $[Cu(\mathbf{L} - 4H)]^{2-}$ with the correct isotopic distribution (100% intensity for the most abundant isotope 228.1, ^{58}Ni and 230.2, ^{63}Cu, respectively). It should be noted, that we succeeded to obtain the mononuclear anionic complexes only in DMSO media (90–95% aqueous DMSO), and use of other solvents did not result in formation of the expected square-planar complexes. The solid complexes $K_2[(Cu(\mathbf{L} - 4H)]\cdot 5H_2O$ (**1**) and $K_2[(Ni(\mathbf{L} - 4H)]\cdot 6H_2O$ (**2**) were isolated by distillation of the solvent *in vacuo*, followed by washing the residues with acetone. Attempts to isolate complexes by addition of nonpolar solvents, slow vapour diffusion or crystallisation *via* metatheses with salts of heavy cations were accompanied by colour changes, suggesting decomposition of the complexes. The colour of the solutions **1** and **2** in DMSO (purple for Cu and orange–yellow for Ni) and position of maxima in electronic spectra are consistent with square-planar complexes and are typical for MN_4 chromophors[7a,13] (508 nm (ε 307 dm^3 mol^{-1} cm^{-1}) for **1** and 423 nm (ε 298 dm^3 mol^{-1} cm^{-1}) for **2**). The EPR spectrum of **1** in DMSO–MeOH glass at 115 K shows superhyperfine structure (nine lines) and is characteristic of in-plane N_4-coordination of Cu^{II} with deprotonated amide

Table 1 Crystal data and structure refinement for **3a**, **3b** and **4**[a]

	3a	**3b**	**4**
Formula	$[Cu_4(C_{20}H_{16}N_8O_2)_2(C_2H_6SO)_2$-$(C_2H_6O)_2](C_6H_2N_3O_7)_4$	$[Cu_4(C_{20}H_{16}N_8O_2)_2(H_2O)_4]$-$(NO_3)_4\cdot 5.5H_2O$	$[Ni_4(C_{20}H_{16}N_8O_2)_2(C_2H_6SO)_6$-$(NO_3)(H_2O)](NO_3)_3\cdot H_2O\cdot 3$-$(C_2H_6SO)\cdot C_3H_6O$
Empirical formula	$C_{72}H_{64}N_{28}O_{36}S_2Cu_4$	$C_{40}H_{51}N_{20}O_{25.5}Cu_4$	$C_{61}H_{96}N_{20}O_{28}S_9Ni_4$
M	2215.79	1474.17	2080.96
Temperature/K	173	293	173
Crystal system	Monoclinic	Hexagonal	Monoclinic
Space group	$C2/c$	$R\bar{3}c$	$P2_1/n$
a/Å	14.3249(7)	29.828(3)	9.3586(5)
b/Å	20.6484(10)		14.3017(8)
c/Å	29.4737(14)	33.759(3)	32.6843(17)
β/°	100.531(1)		90.818(1)
U/Å^3	8571.1(7)	26012(7)	4374(1)
Z	4	6	2
D_c/Mg m^{-3}	1.717	1.694	1.580
μ/mm^{-1}	1.137	1.552	1.149
F(000)	4512	13518	2164
θ range/°	1.41–26.37	2.17–28.34	1.25–28.28
Range hkl	−17 to 17, 0 to 25, 0 to 36	−34 to 0, 0 to 39, 0 to 44	−12 to 12, −19 to 19, −43 to 40
Unique reflections	8732	7214	10666
Data/parameters	5941/651	3345/416	9008/666
Goodness-of-fit on F^2	1.001	0.835	1.156
Final R indices [$I > 2\sigma(I)$]	$R1$[b] = 0.0457, $wR2$[c] = 0.1193	$R1$[b] = 0.0485, $wR2$[c] = 0.1333	$R1$[b] = 0.0810, $wR2$[c] = 0.2071
Final R indices (all data)	$R1$[b] = 0.0750, $wR2$[c] = 0.1316	$R1$[b] = 0.1118, $wR2$[c] = 0.1498	$R1$[b] = 0.0907, $wR2$[c] = 0.2112
Max., min. electron density/e Å^{-3}	1.161, −0.697	1.028, −0.668	1.079, −0.952

[a] Weighting schemes applied: for **3a**: $w = 1/\sigma^2(F_o^2) + (0.0765P)^2$; for **3b**: $w = 1/\sigma^2(F_o^2) + (0.0883P)^2$; for **4**: $w = 1/\sigma^2(F_o^2) + (0.0273P)^2 + 47.8973P$ [where P is defined as $(F_o^2 + 2F_c^2)/3$]. [b] $R1 = \Sigma(F_o - F_c)/\Sigma F_o$. [c] $wR2 = \{\Sigma[w(F_o^2 - F_c^2)^2]/\Sigma[w(F_o^2)^2]\}^{1/2}$.

donors[13] ($g_\perp$ = 2.058, $g_\parallel$ = 2.183, $A_\parallel$ = 207 G). Thus, in the mononuclear complexes **L** acts as a tetradentate open-chain ligand providing four internal nitrogen atoms (two amide and two pyrazole) for in-plane metal coordination and having two vacant bidentate chelating units in close proximity comprising of terminal Py and Pz nitrogens.

At this stage of ligand design, it was not clear whether the mononuclear square-planar complexes (Scheme 2, upper part) would be able to coordinate an extra metal ion with the help of an exterior $\{N(Py), N(Pz)\}_2$ tetradentate compartment forming bi- or tri-nuclear complexes, or the primary square-planar coordination would not be preserved and lead to rearrangement. The first possibility, in the case of binding of one additional metal ion, requires a completely planar conformation of the mononuclear complex anion, however, even in this case the distance between the terminal pyridine nitrogens was estimated to be quite large, so it was expected that the binding of an extra metal ion would be accompanied by severe distortions of the coordination sphere. Binding of two additional metals would require a significant torsion of the aromatic rings out of the interior coordination plane and thus significantly destabilise the primary square-planar coordination thus facilitating realisation of a bis(binucleating) mode.

Indeed, the interaction of copper(II) mononuclear complex **1** with copper(II) salts led to a complete change of the coordination mode of the ligand. Addition of one or two equiv. of copper(II) nitrate to a solution of **1** in DMSO is accompanied by drastic spectral changes which suggest the loss of in-plane CuN_4-coordination and the presence of copper(II) ions in the mixed N,O-donor environment. When one or two equiv. of nickel(II) nitrate is added to the solution of **2** in DMSO, the colour of solution is slowly changes from yellow to light green. Similar changes occur on acidification of the mononuclear complexes. Addition of up to 2.5 equiv. of HCl to a solution of $[Cu(\mathbf{L} - 4H)]^{2-}$ (DMSO–water, 3 : 1 mixture) is accompanied by bathochromic shift of the absorption maximum to 607 nm with a significant decrease in extinction (ε 86 dm^3 mol^{-1} cm^{-1}). Unfortunately, a more detailed solution study of the **L**–Cu system at different pH values was complicated by precipitation of either **L** or Cu-hydroxide in DMSO–water mixtures.

ESI and MALDI mass spectra of solutions obtained from **1** and 2 equiv. of $Cu(NO_3)_2$ show the presence of tetranuclear cations: for the Cu^{II} complex isotopic patterns were detected for $[Cu_4(\mathbf{L} - 2H)_2 - 3H^+]^+$ (100% intensity), $[Cu_4(\mathbf{L} - 2H)_2 - 2H^+]^{2+}$ and $[Cu_4(\mathbf{L} - 2H)_2 - H^+]^{3+}$. Similar species (as minor peaks) were detected in the DMSO solution of Ni^{II} complex **2** to which 2 equiv. of nickel(II) nitrate was added (the 100% intensity peak corresponds to the dimeric $[Ni_2(\mathbf{L} - 4H) + H^+]^+$ species).

The solution of **2** with 2 equiv. of nickel(II) nitrate in DMSO upon exposure to slow diffusion of acetone vapour, produced in several days pale-blue crystals $[Ni_4(\mathbf{L} - 2H)_2(DMSO)_6(NO_3)$-$(H_2O)](NO_3)_3\cdot H_2O\cdot 3DMSO\cdot(CH_3)_2CO$ (**4**). Similarly, the crystalline tetrameric complex $[Cu_4(\mathbf{L} - 2H)_2(DMSO)_2(EtOH)_2]$-$(picrate)_4$ (**3a**) was obtained as a result of slow diffusion of isopropanol to the solution of **1** to which 2 equiv. of copper(II) nitrate and then an ethanol solution of picric acid were added. Thus, tetranuclear complexes **3a** and **4** are formed as a result of the rearrangement of the mononuclear anionic complexes which proceeds on an uptake of extra metal ions and is accompanied by a change of the binding mode of the amide groups (Scheme 2).

The tetranuclear species $[M_4(\mathbf{L} - 2H)_2]^+$ (M = Cu^{2+}, Ni^{2+}) are formed also as a result of metal-induced self-assembly in solution (DMSO or water–acetic acid) containing 1 equiv. of **L** and 2 equiv. of Cu(II) or Ni(II) nitrate. The presence of tetranuclear species is unambiguously detected by ESI and MALDI mass spectrometry. Also, we succeeded in crystallising $[Cu_4$-$(\mathbf{L} - 2H)_2(H_2O)_4](NO_3)_4\cdot 5.5H_2O$ (**3b**) from a solution prepared by addition of $Cu(NO_3)_2\cdot 3H_2O$ (1 mmol) to **L** (0.5 mmol) dissolved in 15 ml of dilute acetic acid (10% in water).

X-Ray single crystal analysis not only confirmed the presence of tetranuclear complex cations and the expected coordination mode of the ligand in both **3a**,**b**§ and **4** but also revealed principal differences in molecular topology of Cu and Ni complexes. Views of the complex cations in **3a**, **3b** and **4** are

§ The bonding parameters in the $[(\mathbf{L} - 2H)_2Cu_4]^{4+}$ core and **3a** and **3b** are very similar. Discussion of structural details will focus on the nitrate salt **3b**.

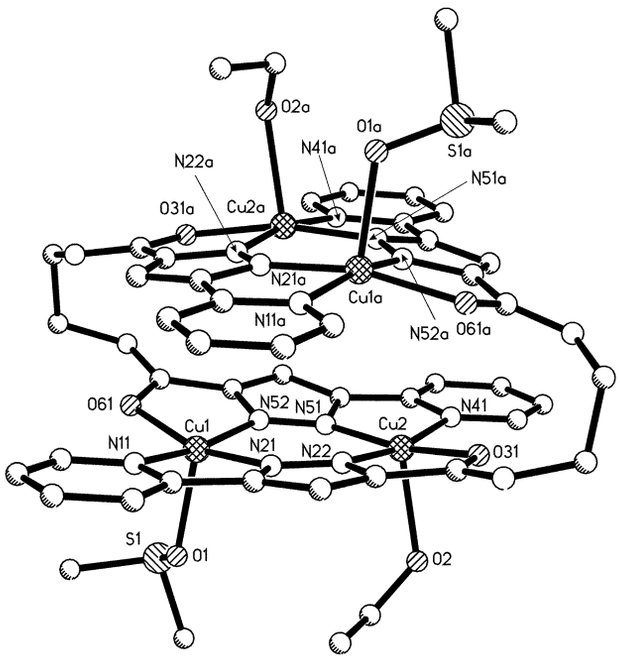

Fig. 1 Molecular structure of the tetranuclear helical complex cation $[Cu_4(\mathbf{L} - 2H)_2(DMSO)_2(EtOH)_2]^{4+}$ in **3a**.

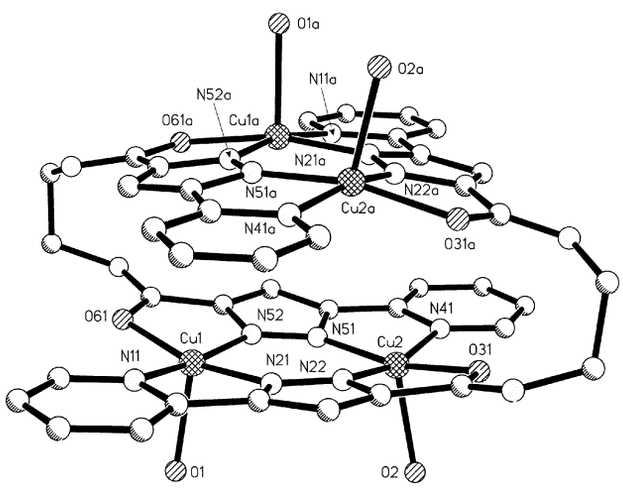

Fig. 2 Molecular structure of the tetranuclear helical complex cation $[Cu_4(\mathbf{L} - 2H)_2(H_2O)_4]^{4+}$ in **3b**.

presented in Fig. 1, 2 and 3, and selected bond lengths and angles for **3a**,**b** and **4** are listed in Tables 2 and 3, respectively. Each complex comprises of two ligand threads which provide donor atoms for in-plane equatorial coordination of four metal ions. In all complexes the ligand is coordinated in bis(binucleating) fashion $(\{N(Py), N(Pz)\}, \{N(Pz), O(amide)\})_2$, forming two pairs of five-membered chelate rings and two bridging pyrazolate groups. However, the ligand threads are disposed in different ways resulting in different topologies in the Cu and Ni complexes (Scheme 2). In **4** two ligands are arranged in a side-by-side manner and are disposed *cis* with respect to the Ni(1)–Ni(2) axis, so that the complex cation consists of two planar decks which are linked in a stair-like fashion by $-NHCH_2$-CH_2NH- groups (Fig. 3). The cation in **4** has crystallographic inversion symmetry with an inversion centre at (1 1/2 0). In contrast, in **3a** and **3b** the ligand threads are disposed *trans* with respect to the Cu(1)–Cu(2) axis and find themselves in a wrapped double helicated conformation (Fig. 1 and 2) which is stabilised by loose interligand Py ⋯ Pz and Py ⋯ Py offset stacking interactions and probably by specific remote Cu ⋯ (η^5)Pz contacts. As a consequence, in **3a** and **3b** all metal ions find themselves in the same equatorial environment

Table 2 Selected bond lengths (Å) and angles (°) for **3a** and **3b**

	3a	**3b**
Cu(1)–N(21)	1.915(3)	1.932(3)
Cu(1)–N(52)	1.928(3)	1.929(3)
Cu(1)–N(11)	2.006(3)	2.030(3)
Cu(1)–O(61)	2.012(2)	2.037(3)
Cu(1)–O(1)	2.209(3)	2.201(4)
Cu(2)–N(22)	1.927(3)	1.926(3)
Cu(2)–N(51)	1.929(3)	1.932(3)
Cu(2)–N(41)	2.017(3)	2.008(3)
Cu(2)–O(31)	2.018(2)	2.017(3)
Cu(2)–O(2)	2.245(3)	2.207(4)
Cu(1) ⋯ Cu(2)	3.9340(6)	3.9556(8)
N(21)–Cu(1)–N(52)	94.05(12)	93.84(13)
N(21)–Cu(1)–N(11)	80.25(12)	79.58(13)
N(52)–Cu(1)–N(11)	167.67(13)	168.31(14)
N(21)–Cu(1)–O(61)	163.74(12)	166.27(13)
N(52)–Cu(1)–O(61)	79.87(11)	79.82(12)
N(11)–Cu(1)–O(61)	102.64(11)	104.43(12)
N(21)–Cu(1)–O(1)	101.60(11)	97.0(2)
N(52)–Cu(1)–O(1)	98.58(12)	97.46(14)
N(11)–Cu(1)–O(1)	93.29(11)	92.95(13)
O(61)–Cu(1)–O(1)	94.24(10)	95.95(18)
N(22)–Cu(2)–N(51)	94.23(12)	93.34(14)
N(22)–Cu(2)–N(41)	169.44(12)	166.38(14)
N(51)–Cu(2)–N(41)	80.05(12)	80.25(13)
N(22)–Cu(2)–O(31)	79.75(11)	80.19(12)
N(51)–Cu(2)–O(31)	167.34(12)	164.35(13)
N(41)–Cu(2)–O(31)	104.04(11)	102.86(12)
N(22)–Cu(2)–O(2)	95.94(12)	100.69(18)
N(51)–Cu(2)–O(2)	102.97(12)	105.14(16)
N(41)–Cu(2)–O(2)	94.00(11)	92.61(16)
O(31)–Cu(2)–O(2)	88.81(10)	90.23(14)

Table 3 Selected bond lengths (Å) and angles (°) for **4**

Ni(1)–N(21)	2.016(5)	N(21)–Ni(1)–N(51)	94.45(19)
Ni(1)–N(51)	2.036(5)	N(21)–Ni(1)–O(2)	94.49(18)
Ni(1)–O(2)	2.099(4)	N(51)–Ni(1)–O(2)	94.92(19)
Ni(1)–O(1)	2.106(4)	N(21)–Ni(1)–O(1)	90.68(19)
Ni(1)–N(11)	2.170(5)	N(51)–Ni(1)–O(1)	96.93(19)
Ni(1)–N(41)	2.184(5)	O(2)–Ni(1)–O(1)	166.66(18)
Ni(2)–N(22)	1.970(5)	N(21)–Ni(1)–N(11)	79.79(18)
Ni(2)–N(52)	1.985(5)	N(51)–Ni(1)–N(11)	171.04(18)
Ni(2)–O(4)	2.095(5)	O(2)–Ni(1)–N(11)	84.02(18)
Ni(2)–O(31)	2.110(4)	O(2)–Ni(1)–N(11)	85.21(17)
Ni(2)–O(3)	2.126(5)	N(21)–Ni(1)–N(41)	169.98(19)
Ni(2)–O(61)	2.134(4)	N(51)–Ni(1)–N(41)	76.18(19)
		O(2)–Ni(1)–N(41)	89.92(18)
Ni(1) ⋯ Ni(2)	4.022(1)	O(1)–Ni(1)–N(41)	86.99(18)
		N(11)–Ni(1)–N(41)	112.68(18)
		N(22)–Ni(2)–N(52)	96.21(19)
		N(22)–Ni(2)–O(4)	94.6(2)
		N(52)–Ni(2)–O(4)	91.5(2)
		N(22)–Ni(2)–O(31)	78.42(18)
		N(52)–Ni(2)–O(31)	174.62(18)
		O(4)–Ni(2)–O(31)	89.30(18)
		N(22)–Ni(2)–O(3)	91.9(2)
		N(52)–Ni(2)–O(3)	89.98(19)
		O(4)–Ni(2)–O(3)	173.1(2)
		O(31)–Ni(2)–O(3)	89.83(18)
		N(22)–Ni(2)–O(61)	173.60(18)
		N(52)–Ni(2)–O(61)	77.38(18)
		O(4)–Ni(2)–O(61)	85.78(19)
		O(31)–Ni(2)–O(61)	107.98(16)
		O(3)–Ni(2)–O(61)	88.00(19)

(CuN_3O), while in **4** Ni(1) and Ni(2) centres reveal two different types of coordination (NiN_4 and NiN_2O_2, respectively). The cations in **3a** and **3b** possesses C_2 crystallographic symmetry (and approaches to the idealised D_3 intrinsic symmetry), and the unit cell contains cations of the opposite helical chirality. However, the two-fold axes in **3a** and **3b** are positioned quite differently. In **3b** the axis passes through the midpoint of the C–C bonds in the diamide linker thus linking two halves of

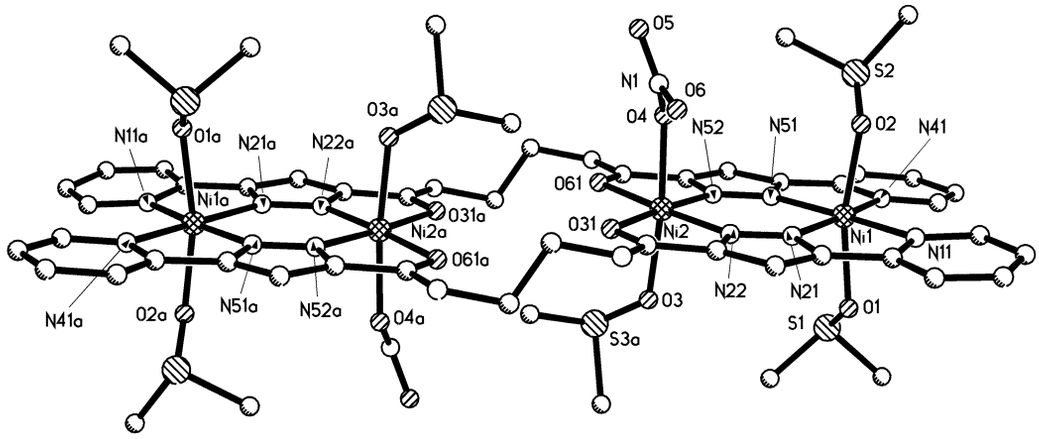

Fig. 3 Molecular structure of the tetranuclear complex cation $[Ni_4(\mathbf{L} - 2H)_2(DMSO)_6(NO_3)(H_2O)]^{4+}$ in **4**.

the molecule. In **3b** the two-fold axis is parallel to the *y* direction of the crystal and situated approximately perpendicular to the vector uniting the midpoins of the C–C bonds of the linkers. To the best of our knowledge, this is the first example of a double helicate comprising of dimeric metal units, so that the helical axis passes not through the metal ions but through the midpoint of the metal–metal vector.

We consider this finding of different topologies in Cu and Ni complexes as a remarkable example of a control of molecular architecture by stereochemical preferences of metal ions. The central cavity of **3b** does not provide enough space for the attachment of the sixth ligand to complete octahedral metal coordination. For this reason a helical structure should be disfavoured with Ni^{2+} ions for which octahedral coordination is preferred in a weak in-plane N_3O ligand field.[14] Indeed, in **4** the Ni^{2+} ions environment is complemented to octahedral by two Ni–O axial contacts with monodentate O-donors (DMSO, water molecules or nitrate anions). In contrast, Cu^{2+} ions in **3a**,**b** adopt a distorted square-pyramidal geometry, typical for Cu^{2+} with N,O-donor set, and compatible with the helical structure in **3**. In our opinion, **3b** and **4** represent a rare case of structurally characterised helical and side-by-side isomers formed by the same ligand with metal ions having different stereochemical preferences. In another reported case, control of topology—helical *versus* non-helical side-by-side—was achieved by subtle modification of ligand structure[2] or by use of metal ions with completely different stereochemical preferences (closed-shell d^{10} ions *versus* octahedral or square-planar open-shell transition metal ions).[15] However, in the latter case Ni^{II} and Pd^{II} ions gave rise to mononuclear planar complexes but not to dinuclear side-by-side isomers of double helical complexes formed by Cu^{I} and Ag^{I} with the tetradentate ligand quaterpyridine (qtpy).[16]

In **3b** the Cu–N(Pz) distances are within the expected range (1.926(3)–2.008(3) Å) and markedly shorter than Cu–N(Py) and Cu–O(amide) bond lengths (2.008(3)–2.030(3) Å and 2.017(3)–2.037(3) Å, respectively) and with long contacts to the apical water (Cu(1)–O(1) 2.201(4), Cu(2)–O(2) 2.207(4) Å). The basal planes of Cu(1) and Cu(2) (defined by three nitrogen and one oxygen donor atoms) are subjected to slight tetrahedral distortion, the copper atoms are displaced towards the coordinated water molecules by 0.200(2) and 0.240(2) Å (for Cu(1) and Cu(2), respectively). The four copper atoms in the tetrameric unit occupy the apices of a distorted polyhedron with Cu ··· Cu distances 3.956(1) Å (in the dimeric unit), 4.653(1), 4.805(1) and 5.033(1) Å (interdimeric distances). As mentioned above, in the cation of **3b** the Py ··· Pz and Py ··· Py stacking interactions with the shortest interatomic contacts N(11) ··· C(54)′ = 3.494(5), N(41) ··· C(24)′ = 3.518(5) and C(13) ··· C(43)′ = 3.441(7) Å (′ indicates the symmetry operation $(-2/3 + y, 2/3 + x, 1/6 - z)$) play an important role in maintaining the helical conformation. These contacts are within the range of distances observed in other reported Cu^{II} complexes with π–π intramolecular aromatic ring stacking.[16] The present structure resembles to a great extent the earlier reported structure $[Cu_4(bPyPz)_4(H_2O)_4](NO_3)_4{\cdot}4H_2O$ (HbPyPz = 3,5-bis(2-pyridyl)pyrazole),[17] where the metal ions and chelating bimetallic pockets are disposed in the same way, however, they belong to four different ligands, so that the structure is not helical. This structure, according to the authors' postulation, is maintained by specific Cu ··· (η⁵)Pz contacts (3.68 Å) which were interpreted as Cu-π(η⁵)Pz bonds.[17] Similar Cu ··· (η⁵)Pz separations were found in **3b** (3.74 and 3.84 Å for Cu(1) and Cu(2), respectively).

Five-membered chelate rings in **3b** differ significantly in their conformation. While the Cu(1)N(52)C(63)C(62)O(61) ring is virtually planar, the other rings are noticeably puckered. The Cu(1)N(11)C(12)C(25)N(21) ring shows an envelope conformation (with the C(12) atom being displaced by 0.120(6) Å from the plane determined by the central and donor atoms), the chelates involving Cu(2) atom indicates chiral conformation (in Cu(2)N(41)C(42)C(55)N(51) the C(42) atom deviates by 0.051(5) Å from the Cu(2)N(41)N(51) plane, in Cu(2)N(22)-C(23)C(32)O(31) the C(23) and C(32) atoms deviate from the Cu(2)N(22)O(31) plane by 0.135(6) and 0.078(6) Å, respectively). The central six-membered ring incorporating two copper atoms exhibits a boat conformation with Cu(1) and Cu(2) displaced from the mean plane defined by four nitrogen atoms by 0.100(6) and 0.153(6) Å, respectively, in the direction of the apical water molecules.

In **4** the Ni(1) octahedron is subjected to tetrahedral distortions in the equatorial plane (alternating deviations of the donor atoms from the mean plane up to 0.05 Å) while Ni(2) forms a perfect plane with the equatorial donor atoms. In both polyhedra significant linear *cis*-distortions are observed: in Ni(1) the Ni(1)–N(Py) distances (2.170(5) and 2.184(5) Å) are markedly longer than Ni(1)–N(Pz) (2.016(5) and 2.036(5) Å) and the axial Ni(1)–O (2.099(4) and 2.106(4)). The Ni(2) octahedron can be described as *cis*-compressed: both Ni(2)–O(amide) and Ni(2)–O(axial) distances are nearly equal (2.110(4), 2.134(4) and 2.095(5), 2.126(5) Å, respectively) while Ni(2)–N(Pz) are much shorter (1.970(5) and 1.986(5) Å). The Ni ··· Ni separation in the dimeric units is 4.022(1) Å. While the five-membered chelate rings in **4** are planar the six-membered chelate ring Ni(1)N(21)N(22)N(51)N(52)Ni(2) exhibits a boat conformation with Ni(1) and Ni(2) atoms ascending by 1.209(4) and 1.354(3) Å, respectively, above the mean plane defined by the nitrogens. The angle between the terminal *cis*-situated Py rings is 9.5(4)°, and the separation between the proximal protons is 2.27 Å and corresponds to the van der Waals contact distance.

In all the structures **3a**,**b** and **4** the tetranuclear complex cations are linked with other elements of the structures (non-coordinated nitrate or picrate anions and solvate molecules) by

multibranched systems of H-bonds. There are no other specific intermolecular contacts in the structures, so that one can conclude that the packing forces play no noticeable contribution in realisation of specific molecular architectures observed in the complex cations of **3a**,**b** and **4**.

The complexes **3b** and **4** were subjected to magnetic susceptibility measurements in the temperature range 1.7–300 K and plots of χ *vs.* T are presented in Fig. 4(a) and (b), respectively.

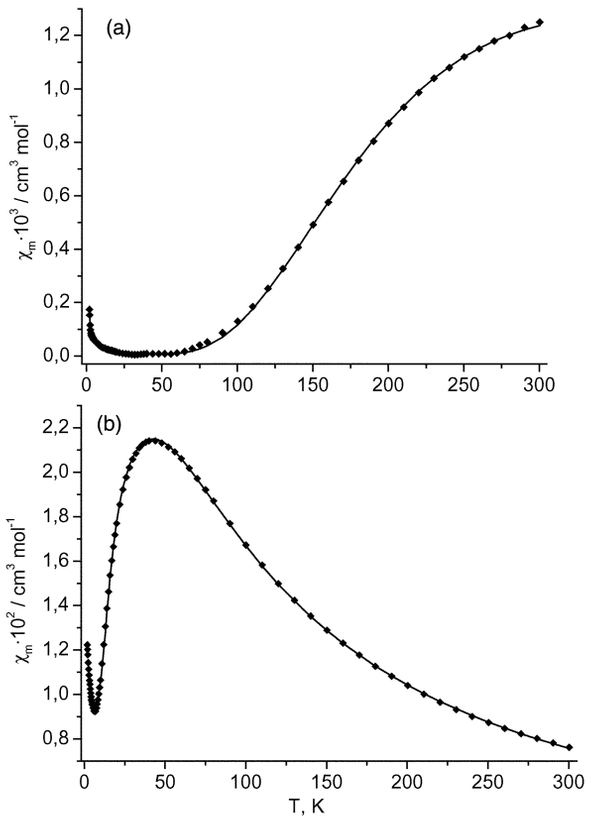

Fig. 4 Temperature dependence of molar magnetic susceptibility per two metal ions χ_m (◆) of a powdered sample of **3b** (a) and **4** (b) with the calculated values (solid lines) based on the parameters given in the text.

The room temperature value of the χT product (0.376 cm^3 K mol^{-1}) for **3b** is much smaller than expected for uncoupled spins and are indicative of strong aniferromagnetic coupling within the dimeric units; χ drops rapidly on cooling and below 60 K complete pairing is in fact achieved, the μ_{eff} values (per Cu atom) are 1.23 μ_B at 300 K and 0.04 μ_B at 50 K.

The magnetic behaviour of **3b** was analysed with the help of modified Bleaney–Bowers expression[18] for two local Cu^{II} ions (eqn. (1)):

$$\chi_m = (2N\beta^2g^2/kT)[3 + \exp(-2J/kT)]^{-1}(1 - \rho) + \rho(2N\beta^2g^2S(S + 1)/3kT + 2N_\alpha \quad (1)$$

where $2J$ is the singlet–triplet energy gap, g the average g factor, $2N_\alpha$ refers to the temperature-independent paramagnetism and N, β, k and T have their usual meanings, ρ is the molar fraction of paramagnetic impurity present in the sample. Since in ref. 17 it was shown that the possible interdimeric cross-interactions within Cu_4 tetramers of similar topology is negligibly small, this factor was not taken into account. Fitting of the experimental data with the least-squares technique (all the parameters were allowed to vary) gave $J = -201$ cm^{-1}, $g = 2.21$ and $\rho = 0.00035$ with $R = 3.05 \times 10^{-4}$ (where R is the agreement factor defined as $R = \Sigma_i((\chi_{obsd})_i - (\chi_{calc})_i)^2/\Sigma_i(\chi_{obsd})_i^2$), as is shown in Fig. 4(a). The general shape of the susceptibility curve is very similar to those reported for tetrameric copper(II) complexes with Pz-bridged ligands.[16,17,19] However, the found J value is higher than those observed in other reported copper(II) tetrameric complexes with HbPyPz ligands where J reaches only $-(160–180)$ cm^{-1} in the case when the exchange interaction is propagated only *via* pyrazolate bridges ($-(162–204)$ cm^{-1} in the case of the presence of both pyrazolato and monoatomic halogenide bridges).[19] This difference can be explained it terms of the presence of the amide oxygen in the coordination sphere of Cu in **3b**. The amide group probably improves the efficiency of superexchange compared to the symmetric HbPyPz ligands. Similarly to the other tetrameric Cu^{II} complexes, the susceptibility of **3b** slightly increases again at lower temperatures (<3 K), which is presumably due to the presence of a small amount of monomeric paramagnetic impurities.[17]

Complex **4** shows an expected value of magnetic moment for uncoupled nickel(II) ions (3.03 μ_B per Ni ion) at 300 K. On cooling, it slowly drops to 2.53 μ_B at 90 K, and below 80 K it decreases more steeply reaching 0.30 μ_B at 1.9 K. The curvature of the temperature dependence of χ_m (Fig. 4(b)) is characteristic of moderate antiferromagnetic interaction: it obeys the Curie–Weiss law between 300 and 80 K (with $\theta = -66$ K), reaches a maximum at 40 K and then drops steeply reaching a minimum at 6.5 K. The susceptibility data were fitted by a modified expression (eqn. (2)) based on the isotropic Heisenberg model[20] ($\boldsymbol{H} = -2J \times \boldsymbol{S}_1 \times \boldsymbol{S}_2$; $\boldsymbol{S}_1 = \boldsymbol{S}_2 = 1$):

$$\chi_m = (N\beta^2g^2/kT)[2\exp(2J/kT) + 10\exp(6J/kT)][1 + 3\exp(2J/kT) + 5\exp(6J/kT)]^{-1}(1 - \rho) + 2\rho(N\beta^2g^2S(S + 1)/3kT + 2N_\alpha \quad (2)$$

The data were very well fitted in the 8–300 K region with $J = -15.8$ cm^{-1}, $g = 2.15$, $\rho = 0.028$ and $R = 5.83 \times 10^{-5}$ in the best fit. The obtained value of J is very close to those observed in other pyrazolato-bridged dinickel(II) complexes,[5a,21] however, in the present case (a double pyrazolate bridge) exchange seems to be more efficient then in reported cases when two nickel ions are mediated by one pyrazolate and one chloride bridges.[5a] Magneto-structural correlations in the latter case revealed a dependence of the J value on the Ni ··· Ni separation: J was found to be $-(12.0–13.1)$ cm^{-1} at a Ni ··· Ni separation of 3.823 Å and dropped to -8.1 cm^{-1} upon lengthening to 3.903 Å. In **4**, this separation is notably larger (4.022(1) Å) but exchange is more efficient. Below 5 K, the susceptibility starts to increase (Fig. 4(b)) due to the presence of a small amount of monomeric paramagnetic impurities.[17]

Conclusions

We reported here a novel polynucleating ligand primary designed for preparation of sterically strained bi- or tri-nuclear complexes but in the course of synthetic studies it revealed an unusual coordinational versatility. Reactions of its mononuclear anionic Ni^{II} and Cu^{II} complexes with metal salts result not in metal binding by the vacant exterior chelate units but in complete change of coordination mode of the ligand (Scheme 2). In our opinion, such behaviour can be attributed to the unfavourable mutual disposition of the face-to-face situated free bidentate units in the ligand **L**, which is not favourable for chelation of either one or two additional metal ions. By contrast, mononuclear Cu^{II} and Ni^{II} complexes of ligands with shorter or longer separation between the exterior chelate units (*e.g.*, carrying 4,6-pyrimidine instead of pyrazolyl substituents) are ideal for binding of one or two exogenous metal ions, respectively, and they form very stable corresponding complexes.[22] However, we still do not exclude the possibility of isolation of anticipated bi- or tri-nuclear complexes of **L** with preservation of the square-planar core, in particular, if using larger or kinetically inert metal ions in the internal site.

Also, we described a simple case of topology control in polynuclear complexes by coordination preferences of the metal ion—helical *versus* side-by-side structure (Scheme 3). The

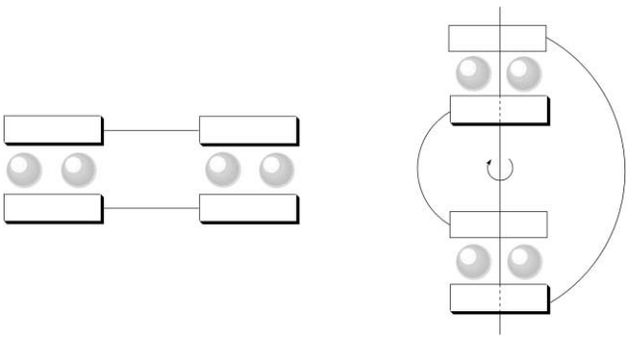

Scheme 3 Schematic representation of topologies in Cu and Ni tetranuclear complexes **3b** and **4**.

reported Ni^{II} and Cu^{II} tetranuclear complexes also demonstrate a possibility to introduce magnetically coupled dimeric units into helicates and other specific molecular arrays. This approach can be expanded to longer ligand strands having more than two dinucleating subunits (in the case of helicates this requires square-planar metals). Important, that Cu^{II} tetranuclear helicate complexes **3a** and **3b** are formed as a result of both metal-induced self-assembly (**3b**) and by the reorganisation of mononuclear matrix on uptake of the additional metal (**3a**). Also, the topology of **3a** and **3b** is more closely related than other helicates to double stranded DNA, since the dinuclear subunits mimic the stacking of nucleobases.

Acknowledgements

This work was funded by the DFG (Gerhard Hess-Programm). We also thank Prof. Dr W. Tremel and S. Stauf, Universität Mainz, for collecting X-ray data for **3b**.

References

1 (*a*) J.-M. Lehn, *Supramolecular Chemistry, Concepts and Perspectives*, VCH, Weinheim, 1995; (*b*) E. C. Constable, in *Polynuclear Transition Metal Helicates*, ed. J.-P. Sauvage and M. W. Hosseini, Pergamon, Oxford, 1996; (*c*) C. Piguet, G. Bernardinelli and G. Hopfgartner, *Chem. Rev.*, 1997, **97**, 2005; (*d*) S. Leininger, B. Olenyuk and P. J. Stang, *Chem. Rev.*, 2000, **100**, 853; (*e*) P. E. Kruger, N. Martin and M. Nieuwenhuyzen, *J. Chem. Soc., Dalton Trans.*, 2001, 1966.
2 S. Rüttimann, C. Piguet, G. Bernardinelli, B. Bocquet and A. F. Williams, *J. Am. Chem. Soc.*, 1992, **114**, 4230.
3 P. L. Caradoc-Davies, L. R. Hanton and K. Lee, *Chem. Commun.*, 2000, 783 and refs. therein.
4 (*a*) I. O. Fritsky, R. Ott and R. Krämer, *Angew. Chem.*, 2000, **112**, 3403; I. O. Fritsky, R. Ott and R. Krämer, *Angew. Chem., Int. Ed.*, 2000, **39**, 3255; (*b*) R. Krämer and I. O. Fritsky, *Eur. J. Org. Chem.*, 2000, 3505; (*c*) I. O. Fritsky, R. Ott, H. Pritzkow and R. Krämer, *Chem. Eur. J.*, 2000, **7**, 1221.
5 (*a*) M. Konrad, F. Meyer, K. Heinze and L. Zsolnai, *J. Chem. Soc., Dalton Trans.*, 1998, 199; (*b*) F. Meyer, I. Hyla-Kryspin, E. Kaifer and P. Kircher, *Eur. J. Inorg. Chem.*, 2000, 771; (*c*) F. Meyer, E. Kaifer, P. Kircher, K. Heinze and H. Pritzkow, *Chem. Eur. J.*, 1999, **5**, 1617; (*d*) F. Meyer, M. Konrad and E. Kaifer, *Eur. J. Inorg. Chem.*, 1999, 1851.
6 (*a*) J. C. Jeffery, P. L. Jones, K. L. V. Mann, E. Psillakis, J. A. McCleverty, M. D. Ward and C. M. White, *Chem. Commun.*, 1997, 175; (*b*) J. S. Fleming, K. L. V. Mann, S. M. Couchman, J. C. Jeffery, J. A. McCleverty and M. D. Ward, *J. Chem. Soc., Dalton Trans.*, 1998, 2047; (*c*) R. L. Paul, S. M. Couchman, J. C. Jeffery, J. A. McCleverty, Z. R. Reeves and M. D. Ward, *J. Chem. Soc., Dalton Trans.*, 2000, 845; (*d*) K. Singh, J. R. Long and P. Stavropoulos, *J. Am. Chem. Soc.*, 1997, **119**, 2942; (*e*) K. Singh, J. R. Long and P. Stavropoulos, *Inorg. Chem.*, 1998, **37**, 1073; (*f*) K. L. V. Mann, E. Psillakis, J. C. Jeffery, L. H. Rees, N. M. Harden, J. A. McCleverty, M. D. Ward, D. Gatteschi, F. Totti, F. E. Mabbs, E. J. L. McInees, P. C. Reidi and G. M. Smith, *J. Chem. Soc., Dalton Trans.*, 1999, 339; (*g*) R. L. Paul, A. J. Amorosi, P. L. Jones, S. M. Couchman, Z. R. Reeves, L. H. Rees, J. C. Jeffery, J. A. McCleverty and M. D. Ward, *J. Chem. Soc., Dalton Trans.*, 1999, 1563.
7 (*a*) T. Kamiusuki, H. Okawa, E. Kitaura, N. Matsumoto, S. Kida and H. Oshio, *J. Chem. Soc., Dalton Trans.*, 1989, 2077; (*b*) D. Fu, G. Wang and W. Tang, *Gaodeng Xuexiao Huaxue Xuebao*, 1992, **13**, 149; (*c*) N. Saha, D. Bhattacharyya and D. Mukherjee, *Inorg. Chim. Acta*, 1986, **125**, 213.
8 W. Gaade, *Recl. Trav. Chim. Pays-Bas*, 1936, **55**, 324.
9 G. M. Sheldrick, SADABS, Program for Scaling and Correction of Area Detector Data, University of Göttingen, Germany, 1996.
10 G. M. Sheldrick, SHELXS-97, Program for Crystal Structure Solution, University of Göttingen, Germany, 1997.
11 G. M. Sheldrick, SHELXTL, Version NT V. 5.1., Bruker AXS, Madison, WI, USA, 1998.
12 (*a*) L. Horwitz, *J. Am. Chem. Soc.*, 1953, **75**, 4060; (*b*) Yu. S. Andreichikov, S. P. Tendryakova, Yu. A. Nalimova, S. G. Pitirimova and L. A. Voronova, *Russ. J. Org. Chem. (Engl. Transl.)*, 1977, **13**, 483.
13 (*a*) A. Dobosz, N. M. Dudarenko, I. O. Fritsky, T. Glowiak, A. Karaczyn, H. Kozlowski, T. Yu. Sliva and J. Swiatek-Kozlowska, *J. Chem. Soc., Dalton Trans.*, 1999, 743; (*b*) A. M. Duda, A. Karaczyn, H. Kozlowski, I. O. Fritsky, T. Glowiak, E. V. Prisyazhnaya, T. Yu. Sliva and J. Swiatek-Kozlowska, *J. Chem. Soc., Dalton Trans.*, 1997, 3853; (*c*) T. Yu. Sliva, A. M. Duda, T. Glowiak, I. Fritsky, V. M. Amirkhanov, A. A. Mokhir and H. Kozlowski, *J. Chem. Soc., Dalton Trans.*, 1997, 273.
14 (*a*) L. Sacconi, F. Mani and A. Bencini, in *Comprehensive Coordination, Chemistry*, ed. G. Wilkinson, R. D. Gillard and J. A. McCleverty, Pergamon Press, Oxford, New York, Beijing, Frankfurt, 1987, vol. 5, pp. 1–347; (*b*) E. Uhlig, *Coord. Chem. Rev.*, 1973, **10**, 227.
15 E. C. Constable, S. M. Elder, M. J. Hannon, A. Martin, P. R. Raithby and D. A. Tocher, *J. Chem. Soc., Dalton Trans.*, 1996, 2423.
16 M. Munakata, L. Ping Wu, M. Yamamoto, T. Kuroda-Sowa, M. Maekawa, S. Kawata and S. Kitagawa, *J. Chem. Soc., Dalton Trans.*, 1995, 4099 and refs. therein.
17 J. Pons, X. Lopez, J. Casabo, F. Teixidor, A. Caubet, J. Ruis and C. Miravitlles, *Inorg. Chim. Acta*, 1992, **195**, 61.
18 B. Bleaney and K. D. Bowers, *Proc. R. Soc. London A*, 1952, **214**, 451.
19 J. Pons, F. J. Sanchez, A. Labarta, I. Casabo, F. Teixidor and A. Caubet, *Inorg. Chim. Acta*, 1993, **208**, 167.
20 C. J. O'Connor, *Prog. Inorg. Chem.*, 1982, **29**, 203.
21 P. W. Ball and A. B. Blake, *J. Chem. Soc. A*, 1969, 1415.
22 I. O. Fritsky, R. Krämer and H. Pritzkow, unpublished results.